CISM COURSES AND LECTURES NO. 493
INTERNATIONAL CENTRE FOR MECHANICAL SCIENCES

WIND EFFECTS ON BUILDINGS AND DESIGN OF WIND-SENSITIVE STRUCTURES

EDITED BY

TED STATHOPOULOS
CHARALAMBOS C. BANIOTOPOULOS

SpringerWienNewYork

SpringerWien NewYork

CISM COURSES AND LECTURES

The series presents lecture notes, monographs, edited works and proceedings in the field of Mechanics, Engineering, Computer Science and Applied Mathematics.
Purpose of the series is to make known in the international scientific and technical community results obtained in some of the activities organized by CISM, the International Centre for Mechanical Sciences.

INTERNATIONAL CENTRE FOR MECHANICAL SCIENCES

COURSES AND LECTURES - No. 493

WIND EFFECTS ON BUILDINGS AND DESIGN OF WIND-SENSITIVE STRUCTURES

EDITED BY

TED STATHOPOULOS
CONCORDIA UNIVERSITY, MONTREAL, QC, CANADA

CHARALAMBOS C. BANIOTOPOULOS
ARISTOTLE UNIVERSITY OF THESSALONIKI, GREECE

SpringerWienNewYork

This volume contains 131 illustrations

Printed in Italy
SPIN 12076963

All contributions have been typeset by the authors.

ISBN 978-3-211-73075-1 SpringerWienNewYork

PREFACE

Aeolos was the Treasurer of the winds. Although he was not a God and had no temples in Ancient Greece, Aeolos is very often met in the Greek mythology and in the early Greek texts. In Odyssey, Odysseus (Ulysses) during his long trip back home to Ithaca, arrived to the island of Aeolos, a floating island close to Sicily. In the caves of this island the winds were imprisoned and Aeolos, following what Gods were dictating to him, used to let them out as soft breezes, gales, storms or whatever Gods wished… Aeolos entertained Ulysses for a whole month, and on Odysseus' departure, gave him as present, a bag containing all adverse winds to hold tight until he went home, so that Odysseus might reach Ithaca with a fair wind. Odysseus did as Aeolos advised him. However, approaching his homeland and while he was sleeping, his men wickedly opened the bag (thinking it was full of gold and silver), allowing all adverse winds to escape. The ships were then blown back to Aeolos' isle, and thence to the land of the savage Laestrygonians, far away from the home island...

Clearly the struggle of Ulysses and his men against the wind resembles the efforts of the contemporary structural engineers to dominate the power of wind and design buildings and wind-sensitive structures to be safe but also economical. However, although the effects of wind are extremely important for contemporary structural design, courses in this area are not generally available within the engineering curriculum of most universities around the world at present. Therefore, this book intends to cover the lack of relevant advanced professional training.

The book contains seven chapters written by wind engineering experts. **Chapter 1**, by Theodore Stathopoulos, addresses the fundamentals of wind engineering, wind velocities, turbulence and structure; it emphasizes the interaction of wind with buildings and refers to the difficulties associated with the evaluation of internal pressures, an issue still problematic in the development of contemporary wind standards and codes of practice. **Chapter 2**, written by Chris Geurts and Carine van Bentum, deals with the evaluation of wind loads on buildings experimentally, either in boundary layer wind tunnels or in full scale and makes particular reference to the application of the Eurocode for the evaluation of design wind loads on buildings. **Chapter 3**, by Jeorg Franke, introduces the concepts of Computational Wind Engineering, i.e. the application of Computational Fluid Dynamics (CFD) in wind engineering, for the prediction of wind loads on buildings. This is an emerging field with still several outstanding issues in the application of various simulation techniques and yields results, which may be unrealistic, therefore untrustworthy, in some cases. **Chapter 4**, authored by Ruediger Hoeffer, Mozes Galffy and Hans-Juergen Niemann, refers to the fundamentals of random vibrations of structures when excited by wind, whereas **Chapter 5**, by Giovanni Solari and Federica Tubino, provides a general framework of the dynamic approach to the wind loading of structures and addresses alongwind, crosswind and torsional structural response. Different methodologies are described with discussion on merits and defects, limits and implications, costs and benefits for each. **Chapter 6**, by Claudio Borri and Carlotta Costa, deals with aeroelastic phenomena with applications in bridge aerodynamics and large roof structures with special reference to galloping, torsional divergence and flutter. Finally, **Chapter 7**, written by Charalambos C. Baniotopoulos, addresses structural design questions for specific wind-sensitive structures, namely steel lattice masts, wind turbine towers and aluminum glass fa-

çades. This chapter includes a discussion of various design code recommendations with respect to serviceability, strength and safety criteria.

The editors would like to thank all contributors to this book for the excellence of their work and also extend their sincere appreciation to the CISM General Secretary, Professor Bernhard Schrefler, the CISM Rector, Professor Giulio Maier, the Editor of the Series Professor P. Serafini, as well as to all CISM staff in Udine for their excellent cooperation.

The book will be of interest for engineers, researchers and academicians who work on relevant scientific research or design topics in research centers, universities, industry and government agencies. The book is written to address the interests of practicing engineers and professionals as well.

The Editors

STATHOPOULOS T.

Concordia University
Montreal, Canada

BANIOTOPOULOS C.C.

Aristotle University of Thessaloniki
Thessaloniki, Greece

CONTENTS

Introduction to Wind Engineering, Wind Structure, Wind-Building Interaction

Theodore Stathopoulos

Department of Building, Civil and Environmental Engineering,
Concordia University, Montreal, Canada

Abstract. A brief introduction to wind engineering with the main characteristics of the wind structure are provided. Velocity profiles, turbulence and spectra are described along with the effects of upstream exposure. Wind speed and turbulence models for inhomogeneous upstream exposures are presented along with data comparisons from other sources. The basic elements of wind-building interaction in the time-averaged mode for uniform and boundary layer flows are described, external and internal pressures and forces on buildings with emphasis on design significance are discussed.

1 Introduction

Wind Engineering is best described as the rational treatment of interaction between wind in the atmospheric boundary layer and man and his works on the surface of earth (Cermak, 1975). It comprises a synthesis of knowledge from fluid mechanics, meteorology, structural mechanics, physiology and the like. Although aerodynamics is of central importance, most applications are non-aeronautical in nature. As far as structural engineering is concerned, the evaluation of wind-induced pressure loads on building surfaces, primary and secondary structural systems, and the consequent along wind, across wind and torsional response are clearly the most important applications. Good knowledge of fluid and structural mechanics is the fundamental background necessary for the understanding of details of interaction between wind flow and civil engineering structures or buildings.

The unsteady character of the wind regime, particularly in urban areas, combined with the additional unsteadiness generated by the separated flow after the wind impacts on a building generates highly fluctuating pressures depending on the flow characteristics and the building configuration. Naturally, the wind-induced pressure regime is more complex than the wind flow regime, so its evaluation becomes more cumbersome and analytical techniques fail in most cases. Consequently, boundary layer wind tunnels simulating atmospheric flows have been used and continue to use extensively for the evaluation of wind loads on buildings. Computational approaches have progressed through the last decade but they are still at a level that hesitation prevails when their results are suggested for use in practical applications.

To start with, wind derives its energy from the sun. Solar radiation is strongest at the equator and this produces temperature differences, which in turn produces pressure differences, which create the so-called atmospheric circulations in an effort for nature to show its fairness by opposing to inequities! Additional variations to the atmospheric circulations are caused by

seasonal effects (annual march of sun north and south of the equator), geographical effects (uneven distribution of water and land) and rotation of earth (greater speed at equator than near the poles). There is a great confusion of names characterizing the various wind types. In the category of secondary circulations, the strongest wind is called hurricane and belongs in the tropical cyclones, which derive their energy by the latent heat released my the condensation of water vapor at low latitudes (near the equator). Hurricanes are known as typhoons in the Far East and cyclones in Australia and Indian Ocean. Extratropical cyclones (30-45 km/h) are produced by mountain barriers or by interaction of air masses along fronts.

Local winds have minimal influence on primary and secondary circulations but, regardless, they may have high intensity. Thunderstorms, caused by heavy precipitation (like wall jets) and tornadoes, which are the most powerful winds causing maximum damage, belong in this category.

2 Wind velocity and turbulence

For winds near the ground surface, frictional effects play a significant role. Ground obstructions retard the movement of air close to the ground surface, causing a reduction in wind speed.

At some height above ground, the movement of air is no longer affected by ground obstruction. This height is called gradient height, Z_G, which is a function of ground roughness. The unobstructed wind speed is called gradient wind speed, V_{Z_G} and it is considered to be constant above gradient height.

The power law, which is used by some engineers to represent variation of wind speed with height, is an empirical equation, which for the case of mean speeds takes the form of

$$\frac{V_z}{V_{z_G}} = \left(\frac{Z}{Z_G}\right)^{\alpha} \tag{1}$$

where Z_G and α are functions of ground roughness. Typical values of Z_G and α are given in Table 1, which also includes the gust speed exponent β replacing α in Eq. (1) when gust speeds are used instead of mean speeds roughness length. It may be noticed that exponent β is approximately equal to 60% of the value of α.

The logarithmic law is used by both engineers and meteorologists. It is based on physics of the boundary layer and it is valid in the bottom 20 to 30% of the boundary layer.

$$\overline{V}_Z = 2.5 \cdot u^* \ln\frac{Z}{Z_o} \tag{2}$$

where

Z_o = roughness length – see typical values in Table 1

u^* = friction velocity = $\sqrt{\frac{\tau_o}{\rho}} \cong 1\text{–}2 m/s$ (for extreme winds)

τ_o = shear stress at the ground surface
ρ = air density

Table 1. Typical values of parameters in wind profiles

Terrain category	Terrain description	Gradient height, Z_G *(m)*	Roughness length, Z_o *(m)*	Mean speed exponent α	Gust speed exponent β
1	Open sea, ice, tundra, desert	250	0.001	*0.11*	0.07
2	Open country with low scrub or scattered trees	300	0.03	*0.15*	0.09
3	Suburban areas, small towns, well wooded areas	400	0.3	0.25	0.14
4	Numerous tall buildings, city centres, well developed industrial areas	500	3	*0.36*	0.20

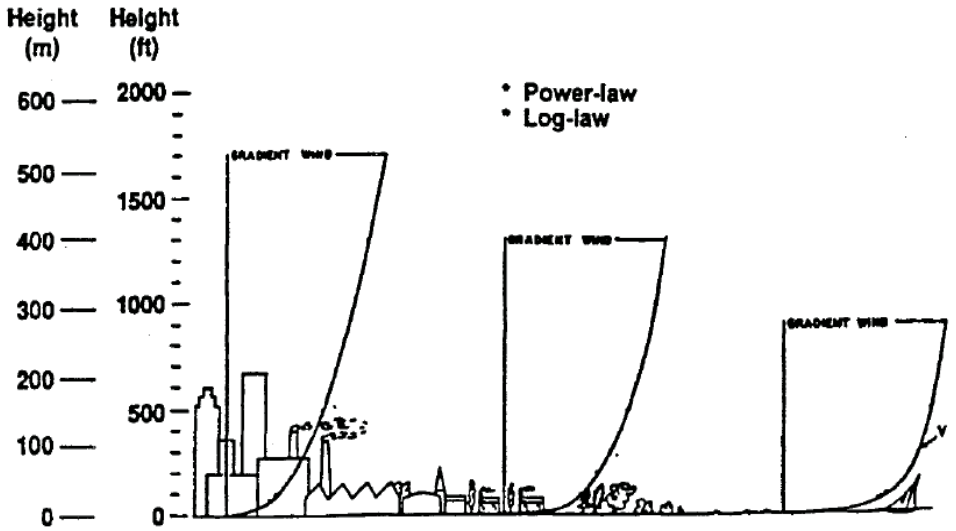

Figure 1. Variation of wind speed with height

Figure 1 shows typical variations of wind speeds above different ground roughness.

Figure 2 shows a typical wind speed variation with time for a 15-minute period. The unsteadiness of the wind is clear. The wind speed can be considered as consisted of two components: mean wind speed and fluctuating component. The fluctuating component, which

is known as turbulence, is caused by convective movement (meteorological) and/or ground roughness (mechanical). In the case of boundary layer flow at high wind speed, it is assumed that mechanical turbulence predominates; this is the case of interest to engineers.

The turbulence (mechanical) is higher in rougher terrain than in smoother terrain, e.g. suburban as opposed to flat open terrain and it decreases with increasing height above ground. The turbulence (gust) parameters of importance are:

- turbulence intensity, defined as

$$Iu = \sigma(z)/U(z) \tag{3}$$

where $U(z)$ = mean wind speed at elevation z and σ = standard deviation value of fluctuating velocity.

- gust size (wind snapshot) referred to as integral scale; and
- gust frequency

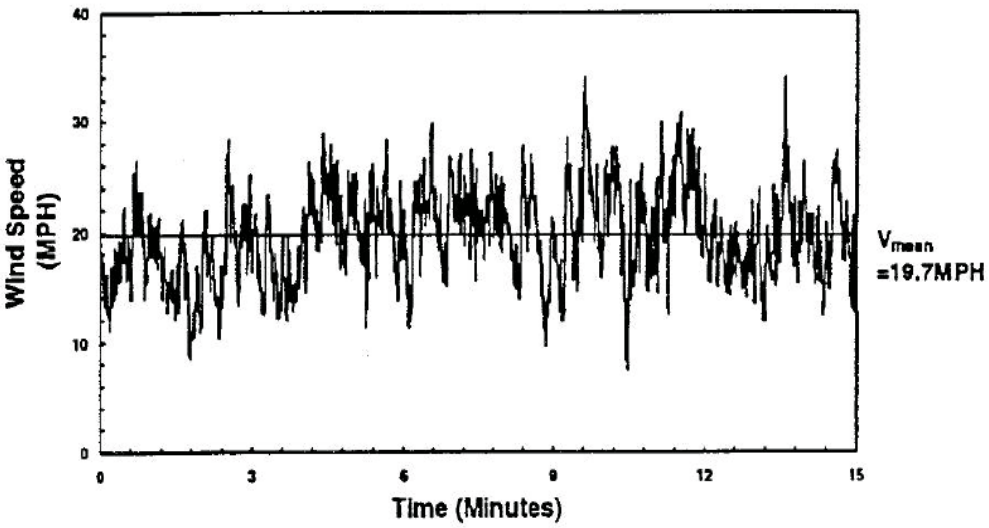

Figure 2. Typical wind speed variation with time

3 Wind structure

Figure 3 shows a typical record of wind velocity obtained from measurements at three different heights of a mast. Stationarity, i.e. the tendency of mean wind speed to stay relatively steady over periods of 10 min to an hour is significant, since it forms the basic idea to wind tunnel testing. The explanation of steadiness lies in the fact that processes generating the mean flow have time scales much, much greater than 1 hour. However, mean speed does vary with time and large fluctuations cover a period of several days.

Some variation in the mean velocity does occur and this is illustrated in Figure 4 by some wind records from a tall tower in Texas. Large fluctuations cover a period of several days, while the speed variation with height is less apparent for some particular days. The variation of wind direction with height is almost nil.

Figure 5 shows the full wind spectrum, as proposed by Van der Hoven (1957). Several distinctive features of the wind speed spectrum have been found from full-scale measurements. Energy appears into two major humps, one at T = 4 days, associated with movement of large scale pressure systems and T = 1 day, related to the diurnal frequency; the other at T = 1 min, associated with turbulence, separated by a gap (T = 10 min to 1 hour), which enables a convenient distinction between "mean wind" and "gusts". The choice of an averaging period for mean wind of 1 hr to 10 min provides fairly stable mean values (thunderstorms may be an exception). It is to be noted that he magnitude of high frequency hump depends on the speed of mean flow.

In addition, it is apparent that wind speed fluctuates randomly at all frequencies. Referring to Fig. 5, the vertical axis represents energy (relative number) at each frequency and the peak is around n = 0.01 Hz (period of 100 seconds). Given that the energy reduces drastically above 1 Hz, wind gusts induce negligible dynamic resonance (buffeting) response to buildings or structures with fundamental frequency greater than 1 Hz.

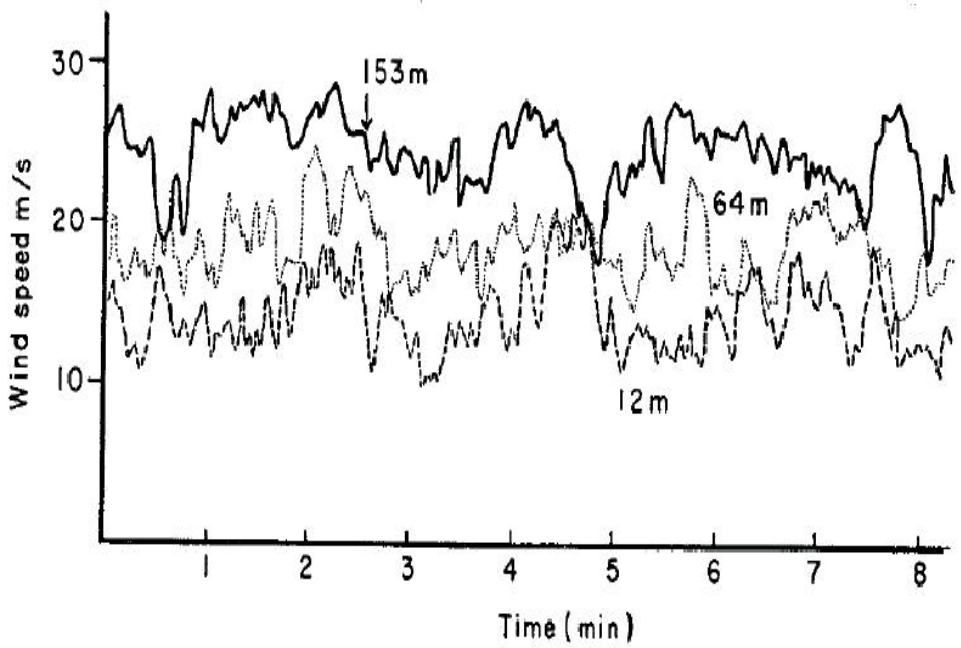

Figure 3. Record of wind speed at three heights on a 153 m mast in open terrain

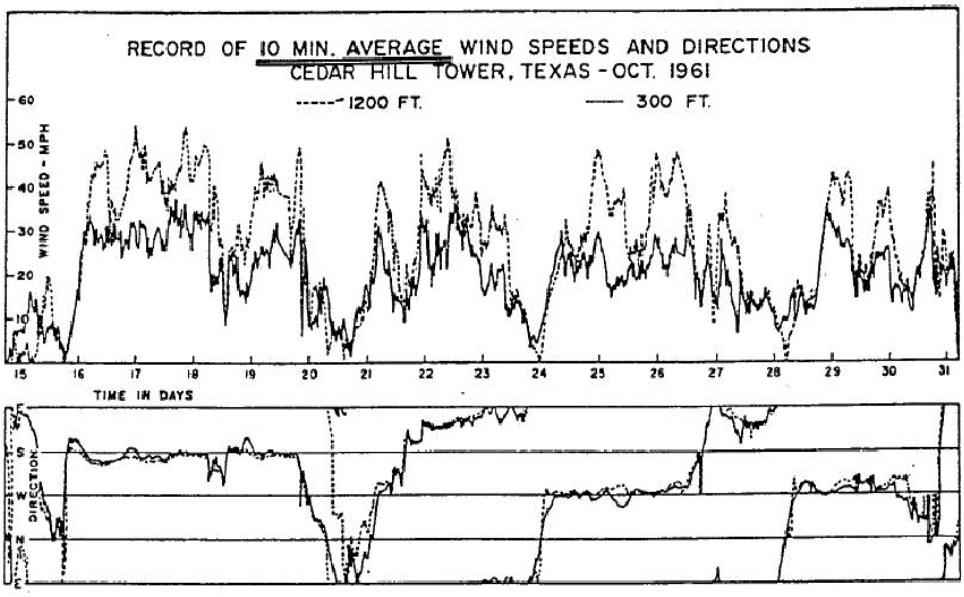

Figure 4. Variation of mean velocity in the atmospheric boundary layer

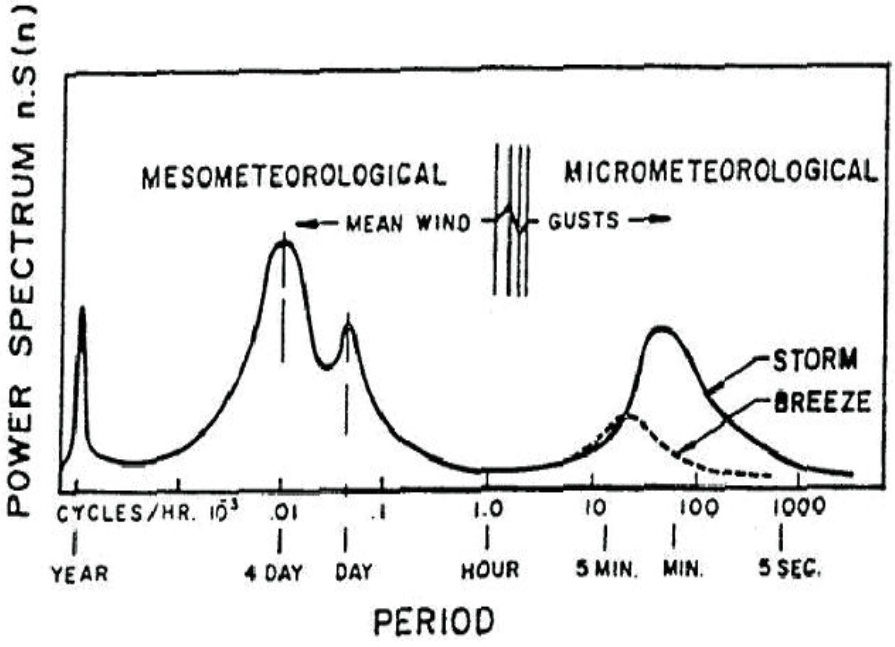

Figure 5. Wind Spectrum, after Van der Hoven (1957)

Figure 6 shows the micrometeorological part of the spectrum, which can be plotted in a smoothed form such as that of Eq. (4), among others, which fits well a series of full-scale data obtained in several locations, as Figure 7 shows.

$$\frac{nS(n)}{k\overline{V}_{10}} = \frac{4.0(\frac{nL}{\overline{V}_{10}})^2}{[1+(\frac{nL}{\overline{V}_{10}})^2]^{4/3}} \tag{4}$$

where

$L \cong 1200$ m

k = surface drag coefficient dependent on the terrain roughness; it has values of about 0.001, 0.005, 0.015 and 0.04 for terrain categories 1-4 (see Table 1) or D-C-B-A respectively

$\overline{V}_{10}$ = mean speed at height of 10 m

Even though mean wind speeds may be lower in a city, gustiness is much higher. In fact, a ratio between the surface drag coefficient in a rough urban area over that in an open terrain is about 10 to 1. Thus in city conditions, the percentage of turbulence in the air speed may be significantly greater.

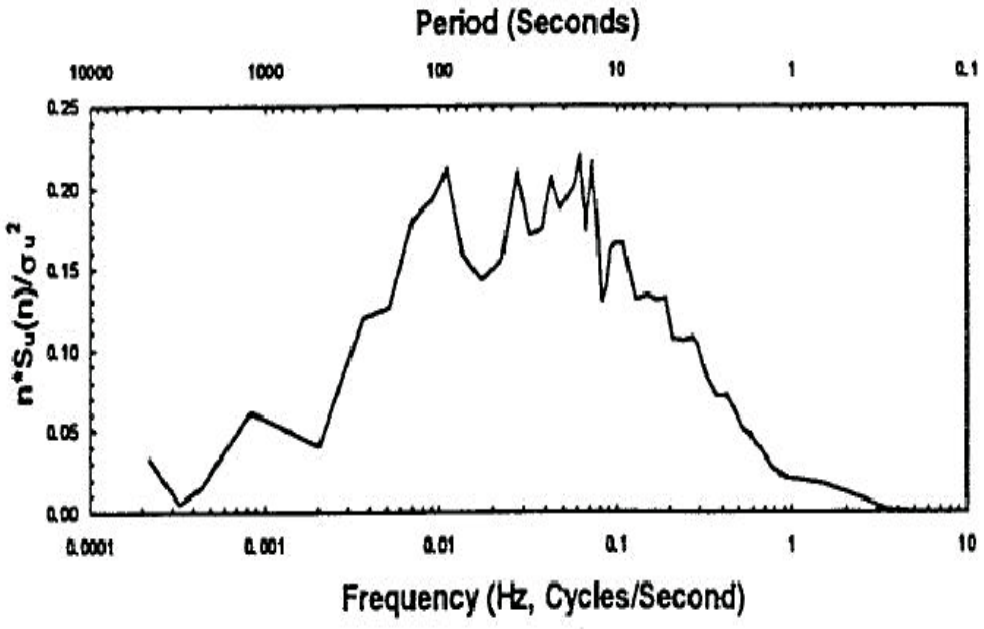

Figure 6. Gust frequency spectrum

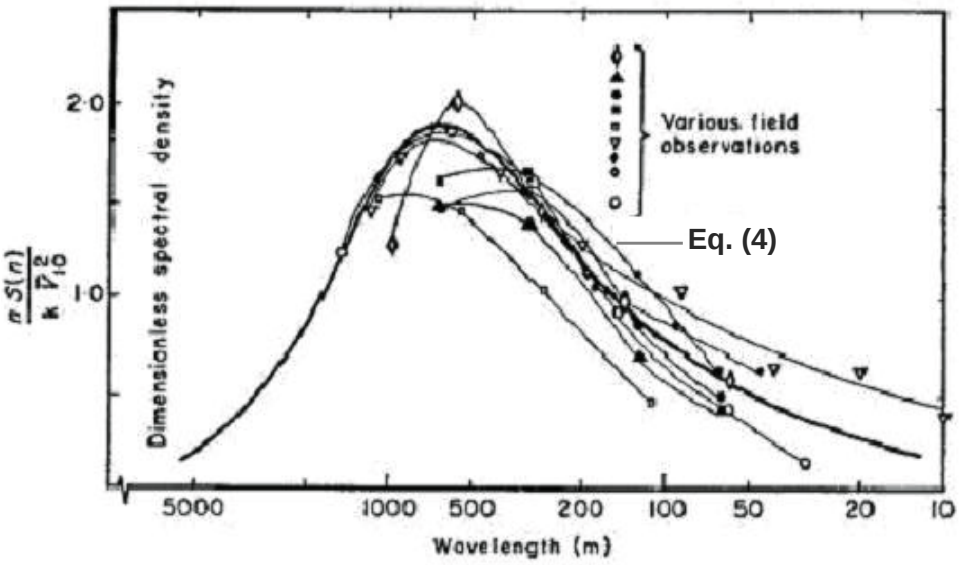

Figure 7. Spectrum of turbulence in strong winds, after Davenport (1967)

4 Upstream exposure

Previous discussion in this chapter addresses mainly upstream exposures with homogeneous roughness. In reality, most practical applications deal with transition cases or mixed upstream exposures, sometimes different for different wind directions as well. Such cases are hard for the design practitioner to handle and codes and standards generally provide little assistance in this regard. Wind speed and turbulence models established recently for such cases are referred to briefly in this section.

4.1 Wind speed model

Recent wind-tunnel investigations confirmed that small-scale roughness changes play an important role on the speed variation above site (Schmid and Bunzli 1995, Zhang and Zhang 2001). Above a well-defined pertinent fetch, the patches may stratify the boundary layer regime into an outer sub-layer or a set of corresponding Internal Boundary Layers (IBL's). The IBL depth growth *g(x)* may be modelled by a 0.8 power law, as mentioned in Garratt (1990), as follows:

$$g(x) \propto z_{o,r}^{0.2} x^{0.8} \tag{5}$$

where $z_{o,r}$ is the greatest of an upstream patch roughness length or its adjacent downstream patch roughness length; x is the distance from the change of roughness to the site. Each

segment in the speed profile is dictated by the power law index of the corresponding patch. An illustrative example is shown in Fig. 8 in order to outline the general features of the model.

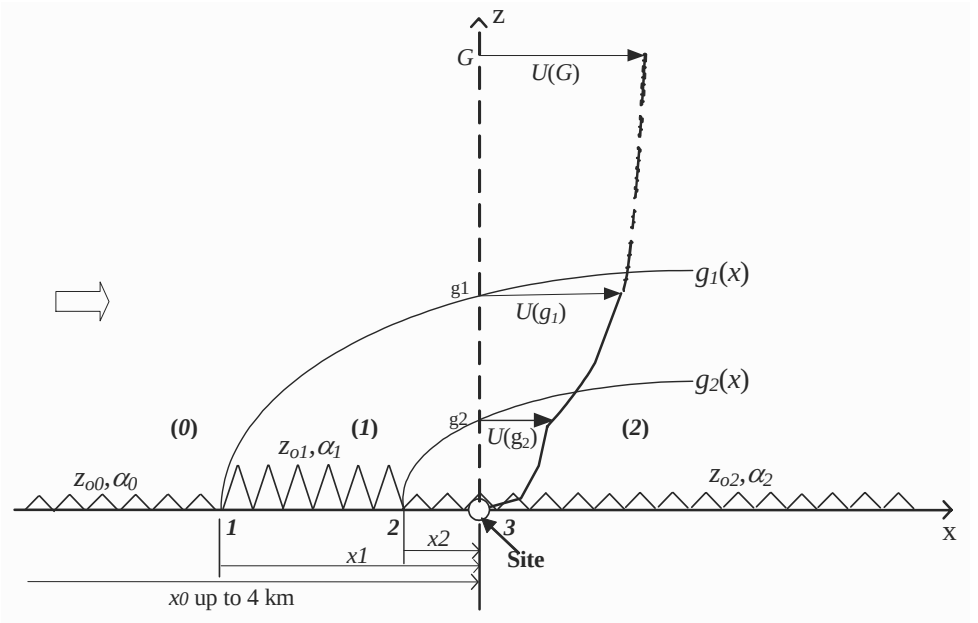

Figure 8. Schematic boundary layer with two IBL's developing above a fetch with two roughness changes

This example has a pertinent fetch of three patches: patch 0 from the 4 km upwind location to the first roughness change location 1; patch 1 from roughness change location 1 to 2; and patch 2 from roughness change location 2 to the site. The entire boundary layer is correspondingly stratified into three sub-layers: outer sub-layer (*0*) in the height range from *G* down to $g_1(x)$, IBL (*1*) from $g_1(x)$ down to $g_2(x)$, and IBL (*2*) from $g_2(x)$ down to the ground. Both $g_1(x)$ and $g_2(x)$ may be modelled with the 0.8 power law (2). The layer depths $g_1(x)$ and $g_2(x)$ break the speed profile at the site into three segments, each of which can be modelled by power-law equation with the patch-respective power-law indices α_o, α_1 and α_2.

The proposed speed model has the form:

Gradient height:

$$g_n(x) = G \quad (n = 0) \tag{6}$$

IBL depth:

$$g_n(x) = 0.5 z_{o,(n,n-1)}^{0.2} x_n^{0.8} \quad (n = 1, 2, \ldots, N) \tag{7}$$

Speed profile segment:

$$U(z) = U\left(g_n(x)\right)\left(\frac{z}{z_{g_n}}\right)^{\alpha_n} \quad (g_{n+1} < z \le g_n;\ n = 0, 1, \ldots, N; \tag{8}$$

in which the subscript n denotes the patch number, i.e., patch N is the patch of the site; $g_o(x)$ denotes the gradient height; $g_n(x)$ denotes the depth of the n^{th} IBL; x_n is the distance from the n^{th} roughness change to the site; $z_{o,n}$ and α_n are roughness characteristic values of patch n; and $z_{o,(n,\,n-1)} = z_{o,n-1}$ or $z_{o,n}$, whichever is larger. For homogeneous terrain of no roughness change, $N = 0$, Eq. (7) does not apply and Eq. (8) reduces to the ordinary power law.

In order to use Eqs. (6) – (8), the boundary conditions need to be specified for the pertinent fetch length, the patch information (x_n, $z_{o,n}$, α_n), the gradient height G, and the gradient wind speed $U(G)$. In this study, the pertinent fetch length is assumed as constant 4 km. Patch roughness information (x_n, $z_{o,n}$, α_n), and the gradient height G for the pertinent fetch can be found in Table 2 after Davenport et al. (2000) and ASCE (1999).

Table 2. Roughness classification after Davenport et al. (2000) with power law α values after ASCE (1999)

Roughness Class	z_o (m)	α	G (m)
1. Sea	0.0002	*0.09*	213
2. Smooth	0.005	*0.125*	213
3. OC	0.03	0.15	274
4. Roughly open	0.1	*0.2*	274
5. Suburban (Rough)	0.25	0.25	366
6. Very rough	0.5	*0.3*	366
7. Urban (Closed)	1	0.33	366

Numbers in *italics* are obtained by best fit of data.

The highest roughness grade (Class 8, Chaotic, $z_o > 2$ m) of the original classification (Davenport et al. 2000) is combined within Urban (Closed) in compliance with ASCE 7-02. Values of $U(G)$ are available in wind standards and codes of practice.

Discussion

The application and validation of this new speed model has been discussed in detail by Wang and Stathopoulos (2005). This section includes an example demonstrating how the proposed model fits the actual ESDU (82026) values for a case of inhomogeneous upstream terrain. The example provided in the ESDU document was deemed the most appropriate case to check. The ESDU (82026) example requires to find the mean speed profile at a site downwind of two changes in surface roughness, given the reference speed $U(10)$ = 22 m/s, and the fetch containing three patches, as shown in Figure 9.

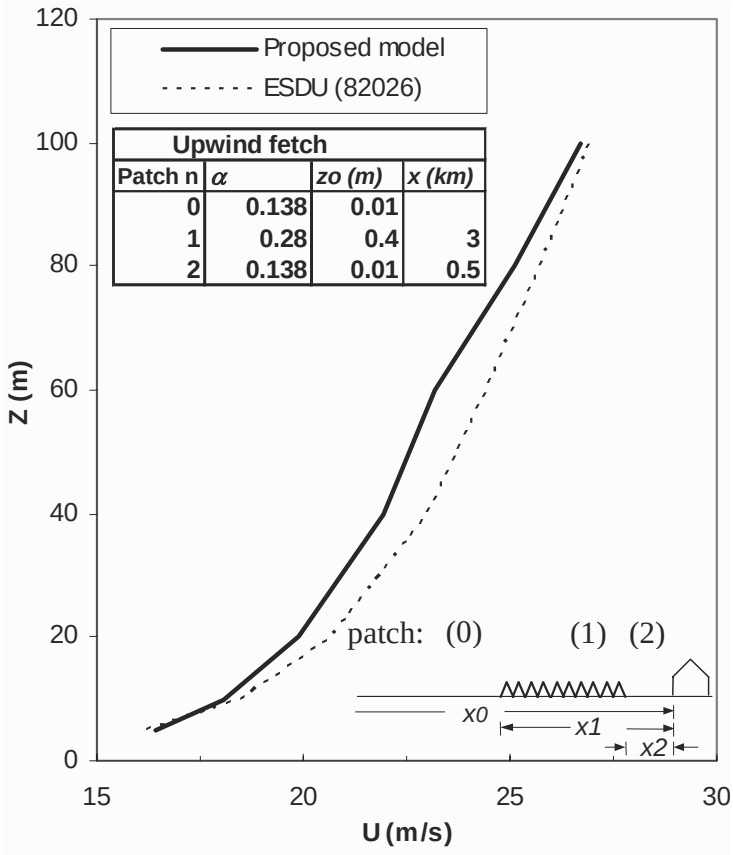

Figure 9. The proposed speed model and the ESDU (82026) model for the ESDU (82026) example case (terrain condition shown), after Wang and Stathopoulos (2005)

ESDU (82026) appears to take a lot more steps than the proposed model in speed profile calculation. It is worth noting that the probability factor, which is taken into account by the original ESDU (82026) data, has been removed in the comparison of Figure 9, which shows that the agreement between the proposed model and ESDU (82026) is reasonable, particularly below 20 m and above 80 m. For intermediate heights, ESDU tends to provide higher values than the proposed model, which thus appears less conservative than ESDU (82026). However, the proposed model agrees better with the full-scale investigation of Letchford et al. (2001) on a geometrically similar fetch configuration under hurricane conditions. It is of interest to note that Letchford et al. (2001) found that the ESDU (82026) transitional speed model may tend to overestimate, by as much as around 20%, the increase in speed at 10 m height induced by an R-S (rough-to-smooth) upstream terrain change. It is also noteworthy that this particular case ensures conditions of neutral atmospheric stability considering the high wind speeds it refers to.

4.2 Turbulence model

Although the detailed derivation of the turbulence model is not presented here, it can be found in Wang and Stathopoulos (2005**).** However, a comparison with the experimental data for a fetch with a single roughness change (from open country to suburban) is shown in Figure 10. The proposed model agrees well with the experimental data, whereas the ESDU (84030) data overestimates the turbulence intensity at higher heights. However, there is excellent agreement among data, ESDU model and the present study results, as well as the ESDU data for heights less than 30 m, i.e. the height zone of most low buildings

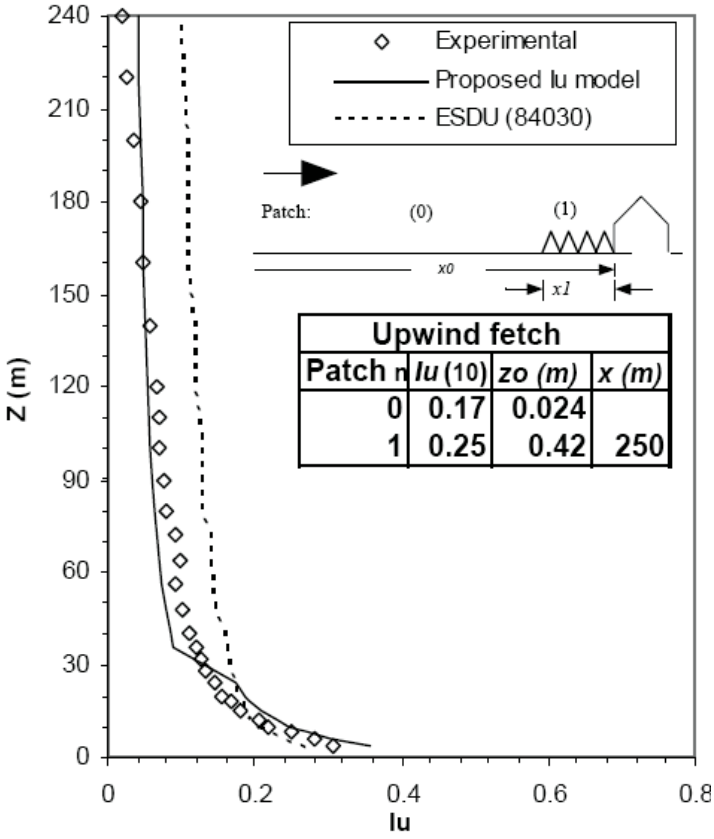

Figure 10. The *Iu* model and wind-tunnel data for a fetch with a single roughness change, and the ESDU (84030) data for a very similar fetch, after Wang and Stathopoulos (2005)

5 Mean wind pressure loads on buildings

Airflow around buildings produces pressure distributions on the building envelope. Knowing these distributions is important in a number of engineering applications. In case of

strong oncoming winds, the flow may produce high negative pressures that can cause damage to cladding of tall buildings or roofs of low buildings, particularly near corners and edges. The distribution of air contaminants exhausted from a building may also be affected even for low or moderate winds, the air infiltration will be altered due to the differences in the internal pressures of the building and the intake and exhaust flow rates will be different causing possible problems to the HVAC system performance.

5.1 Uniform flow conditions

The airflow velocity (V) produces a pressure (P) evaluated by the well known Bernoulli's equation, which for horizontal flows can be written as

$$P + 1/2\,\rho V^2 = constant \tag{9}$$

where the second term is called dynamic pressure and ρ is the air density. This equation is valid for ideal conditions of non-viscous, steady and irrotational flow – see Figure 11 – so it cannot be used in the case of turbulent flows around buildings.

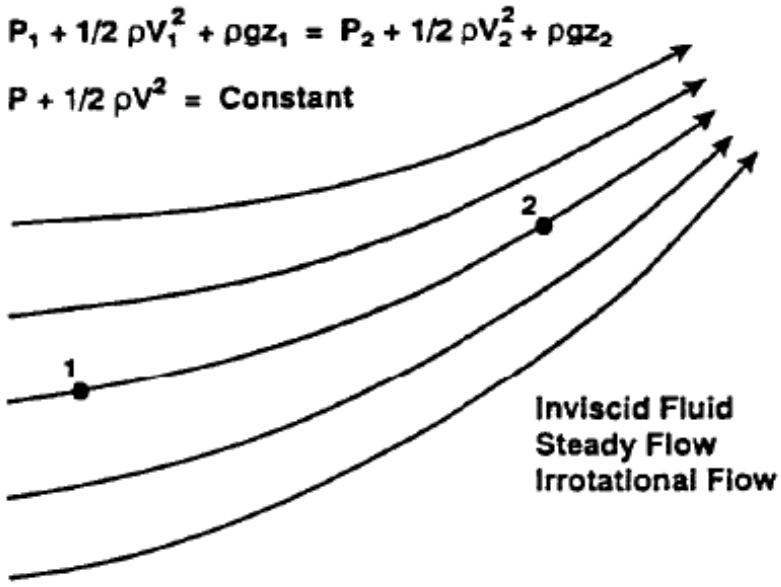

Figure 11. Bernoulli's equation for a streamline

Since most buildings and other civil engineering structures are not streamlined in nature, traditional aerodynamics calls them "bluff bodies". The implication is that wind flow separates and causes the formation of the so-called "wake", see Figure 12 showing the basic characteristics of steady flow around a simple rectangular building or tower. If air was an ideal (non-viscous) fluid, there would not be any separation and Bernoulli's equation would be

applicable in all places. However, as Figure 2 demonstrates, the wind flow separates from the body at the two upstream edges and forms two regions: an outer flow, where there is no viscosity effect (except a very thin layer on the front face of the building) and an inner flow, i.e. the wake region. The outer flow is separated by the inner flow by an area of high vorticity, called "shear layer".

Clearly Bernoulli's equation is only valid in the outer flow region and the constant in Eq. (9) can be evaluated by using the pressure (atmospheric) P_o and velocity of the undisturbed free stream flow V_o to get

$$\Delta P = P - P_o = 1/2\ \rho V_o^2 - 1/2 \rho V^2 \tag{10}$$

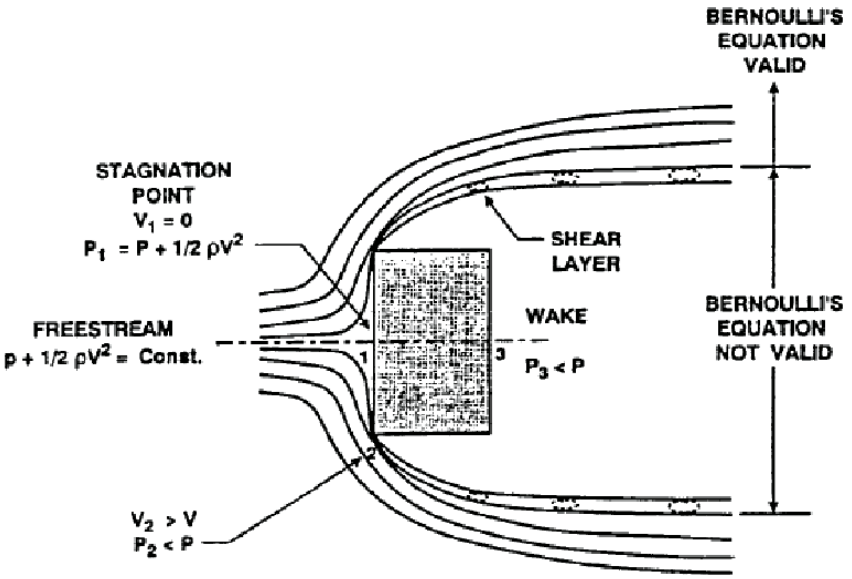

Figure 12. Bernoulli's equation and wind flow around a rectangular building

For ideal conditions of stagnation $V_1 = 0$; $P_1 = P + 1/2\ \rho V^2$
Also, if $V_2 < V$, $P_2 > P$; this implies inward acting pressure (overpressure or simply pressure).
However, if $V_2 > V$, $P_2 < P$, i.e. outward acting pressure, known as suction.
Pressures are usually expressed in a dimensionless form to be independent of velocities. This dimensionless form is called pressure coefficient (C_P) and is defined as follows:

$$C_P = \frac{\Delta P}{1/2 \rho V_o^2} \tag{11}$$

in which ΔP is the pressure induced by wind (above or below ambient atmospheric pressure); commonly ΔP is called P.
Eq. (11) can also be rewritten as:

$$C_P = \frac{P - P_o}{1/2\rho V^2} = [1 - (\frac{V}{V_o})^2] \tag{12}$$

Eq. (12) shows that the pressure coefficient can reach a maximum value of +1 at stagnation points where $V = 0$; thus positive values of C_P close to one are observed on sides of building facing the wind. C_P is 0 in the free stream where $V = V_o$ and negative for values of $V > V_o$. Negative values of C_P are observed on roofs and sides of building.

The wake region in Figure 12 is characterized by little pressure gradient. Bernoulli's equation is not applicable but pressure coefficients can also be expressed in dimensionless form:

$$C_{P_w} = \frac{P_w - P_o}{1/2\rho V_o^2} \tag{13}$$

Pressure coefficients in wake are invariably negative. Typical time series of pressure coefficients along with variation of wind speed and their statistics are shown in Figure 13. Definitions of Cp_{mean} and Cp_{peak} are:

Mean pressure coefficient: $Cp_{mean} = C_P = \frac{\Delta P_{mean}}{1/2\rho V_{mean}^2}$ (14)

Peak pressure coefficient: $Cp_{peak} = GC_P = \frac{\Delta P_{peak}}{1/2\rho V_{mean}^2}$ (15)

The location of separation points and the geometry of the wake have a substantial influence on the pressure distribution and the total forces on the bluff obstacle. In the case of rectangular cylinder the separation points were dictated by the geometry of the prism. The boundary layer, which builds up on the front surface, fails to flow around the sharp corners boundary layer, which builds up on the front surface, fails to flow around the sharp corners and separates. For other bluff shapes particularly for those with curved surfaces such as wires, chimneys, and circular tanks the separation points are not easy to predict. For a circular cylinder, for example, separation takes place at different positions depending on the magnitude of the viscous forces, which dominate the flow within the boundary layer. The relative magnitude of these viscous forces can be expressed in the form of a dimensionless parameter known as the Reynolds number R_e:

$$R_e = \frac{inertia\ forces}{viscous\ forces} \propto \frac{\rho V_o^2 D^2}{\mu \frac{V_o}{D} D^2} \tag{16}$$

Thus $R_e = \frac{V_o D}{\nu}$ (17)

in which ρ is the density, μ is the dynamic viscosity, and ν is the kinematic viscosity of the air.

Figure 14 shows the variation of pressure coefficients on the surface of a circular cylinder for different values of R_e. Clearly the influence on the side face and the leeward side is significant.

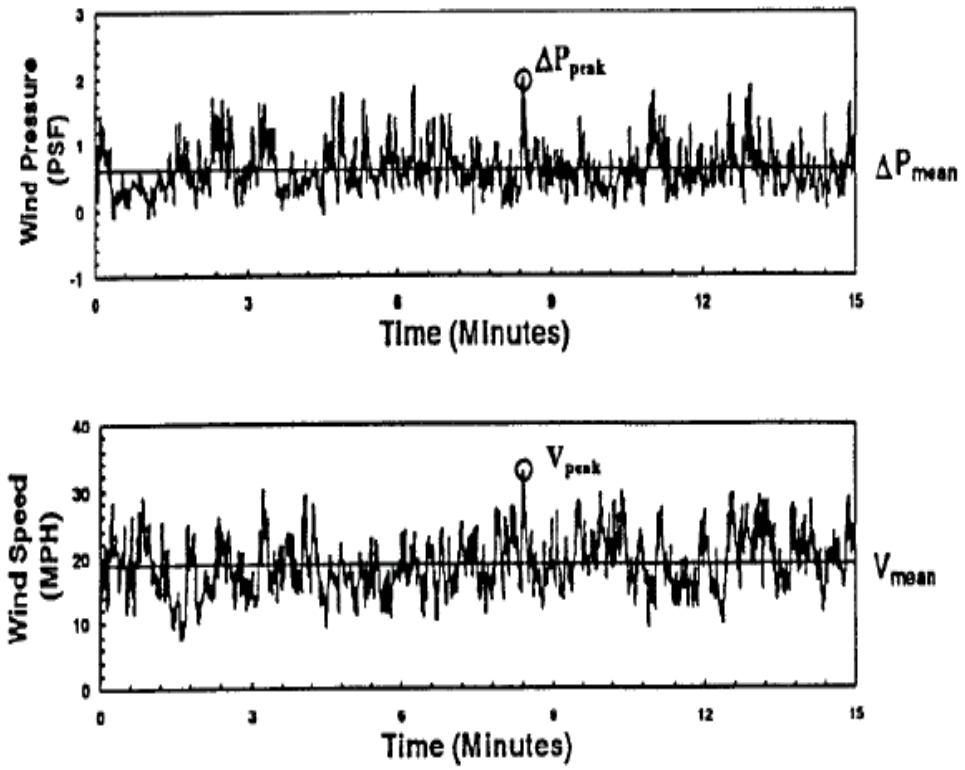

Figure 13. Wind pressure and wind speed traces indicating mean and peak values

The time-averaged aerodynamic forces on structures can be expressed as along wind or drag forces (F_D) and across wind or lift forces (F_L). The latter should not be confused with the upward lift forces acting on horizontal building elements such as roofs. The drag force is normally larger, as far as static loads on buildings is concerned. Both drag and lift forces can be expressed also in terms of coefficient form, as follows:

Drag coefficient $C_D = \frac{F_D}{1/2\rho V_o^2 h}$ (18)